MOLECULAR AND CELLULAR BIOLOGY, Feb. 2003, p. 1034–1043 Vol. 23, No. 3
0270-7306/03/$08.00+0 DOI: 10.1128/MCB.23.3.1034–1043.2003

Loss of S100A9 (MRP14) Results in Reduced Interleukin-8-Induced CD11b Surface Expression, a Polarized Microfilament System, and Diminished Responsiveness to Chemoattractants In Vitro

Marie-Pierre Manitz,[1] Basil Horst,[1] Stephan Seeliger,[1] Anke Strey,[2] Boris V. Skryabin,[3] Matthias Gunzer,[4] Werner Frings,[1] Frank Schönlau,[1] Johannes Roth,[1] Clemens Sorg,[1] and Wolfgang Nacken[1]*

Institute of Experimental Dermatology,[1] Institute of Medical Biochemistry,[2] and Institute of Experimental Pathology,[3] Zentrum für Molekularbiologie der Entzündung, and Department of Dermatology, Ludwig Boltzmann Institute of Cell Biology,[4] University of Münster, 48149 Münster, Germany

Received 15 August 2002/Returned for modification 13 September 2002/Accepted 22 October 2002

The S100A9 (MRP14) protein is abundantly expressed in myeloid cells and has been associated with various inflammatory diseases. The S100A9-deficient mice described here were viable, fertile, and generally of healthy appearance. The myelopoietic potential of the S100A9-null bone marrow was normal. S100A8, the heterodimerization partner of S100A9 was not detectable in peripheral blood cells, suggesting that even a deficiency in both S100A8 and S100A9 proteins was compatible with viable and mature neutrophils. Surprisingly, the invasion of S100A9-deficient leukocytes into the peritoneum and into the skin in vivo was indistinguishable from that in wild-type mice. However, stimulation of S100A9-deficient neutrophils with interleukin-8 in vitro failed to provoke an up-regulation of CD11b. Migration upon a chemotactic stimulus through an endothelial monolayer was markedly diminished in S100A9-deficient neutrophils. Attenuated chemokinesis of the S100A9-deficient neutrophils was observed by using a three-dimensional collagen matrix migration assay. The altered migratory behavior was associated with a microfilament system that was highly polarized in unstimulated S100A9-deficient neutrophils. Our data suggest that loss of the calcium-binding S100A9 protein reduces the responsiveness of the neutrophils upon chemoattractant stimuli at least in vitro. Alternative pathways for neutrophil emigration may be responsible for the lack of any effect in the two in vivo models we have investigated so far.

Two members of the calcium-binding S100 protein family, S100A9 (MRP14) and S100A8 (MRP8), contribute up to 40% of the total cytosolic protein in neutrophils (19). Both proteins form stable heterodimers that are secreted upon stimulation. The S100A9- and S100A8-positive leukocytes belong to the first group of cells invading inflammatory sites and are considered part of the unspecific first line of defense against inflammatory agents. Both proteins are up-regulated in humans during many inflammatory diseases, resulting in increased levels in serum (12). The heterodimer has long been considered to be the active principal. However, recent reports suggest that both proteins may have individual functions and that heterodimerization involves a regulatory process. The S100A9 and S100A8 molecules seem to be involved in the molecular processes leading to adhesion and/or (trans)migration. Murine S100A8 has been identified as a strong chemotactic agent (14) and may act as an antioxidative molecule protecting the inflamed tissue against the oxidative stress generated by neutrophils (23). Extracellular S100A9 modulates the affinity of the Mac-1 integrin receptor via a G-protein-mediated mechanism (21) and may also bind to heparan sulfate (27) and carboxylated proteoglycans (30) located on endothelial cells, facilitating transmigration. Heterodimerization with S100A8 may have a regulatory role in these phenomena.

* Corresponding author. Mailing address: Institute of Experimental Dermatology, Von Esmarch Str. 58, 48149 Münster, Germany. Phone: 49-251-8356552. Fax: 49-251-8356549. E-mail: nacken@uni-muenster.de.

The intracellular functions of both proteins are less well understood. Several reports have described the association of both proteins with cytoskeletal elements; however, the functional relevance of these observations has so far not been shown (26, 32). Furthermore, it was proposed that both proteins are involved in the terminal differentiation of neutrophils by inhibiting casein kinase (18). The mere abundance of both calcium-binding proteins in neutrophils implies a role in the maintenance of calcium homeostasis in these cells.

Recently, S100A8-deficient mice revealed an unexpected role for this molecule in embryogenesis since the S100A8-deficient embryos were resorbed by day 9.5 (22). The death of these animals at the embryonic stage prevented a detailed functional analysis of S100A8 protein in the adult mouse. Here, we describe experiments with S100A9-deficient mice. These mice appear to be phenotypically normal, even in two inflammatory models. Nonetheless, a detailed analysis of the S100A9-null neutrophils revealed a disturbed G/F-actin balance accompanied by a decreased responsiveness to interleukin-8 (IL-8)-mediated CD11b surface recruitment and a reduced migration upon chemoattractant stimulation in vitro.

MATERIALS AND METHODS

Antibodies and cytokines. The following monoclonal antibodies (MAbs) were obtained from BD PharMingen (Heidelberg, Germany): R-phycoerythrin-conjugated rat anti-mouse CD11b (M1/70); fluorescein isothiocyanate (FITC)-conjugated rat immunoglobulin G2a(κ) (IgG2a/k), R35-95; FITC-conjugated rat anti-mouse Ly-6G (Gr1), RB6-8C5; rat anti-mouse CD54R/B220, RA3-6B2; rat anti-mouse Ly-6G (Gr1), RB6-8C5; and rat anti-mouse CD90, Thy-1.2. The following MAbs were also obtained: from BMA (Augst, Switzerland), rat anti-

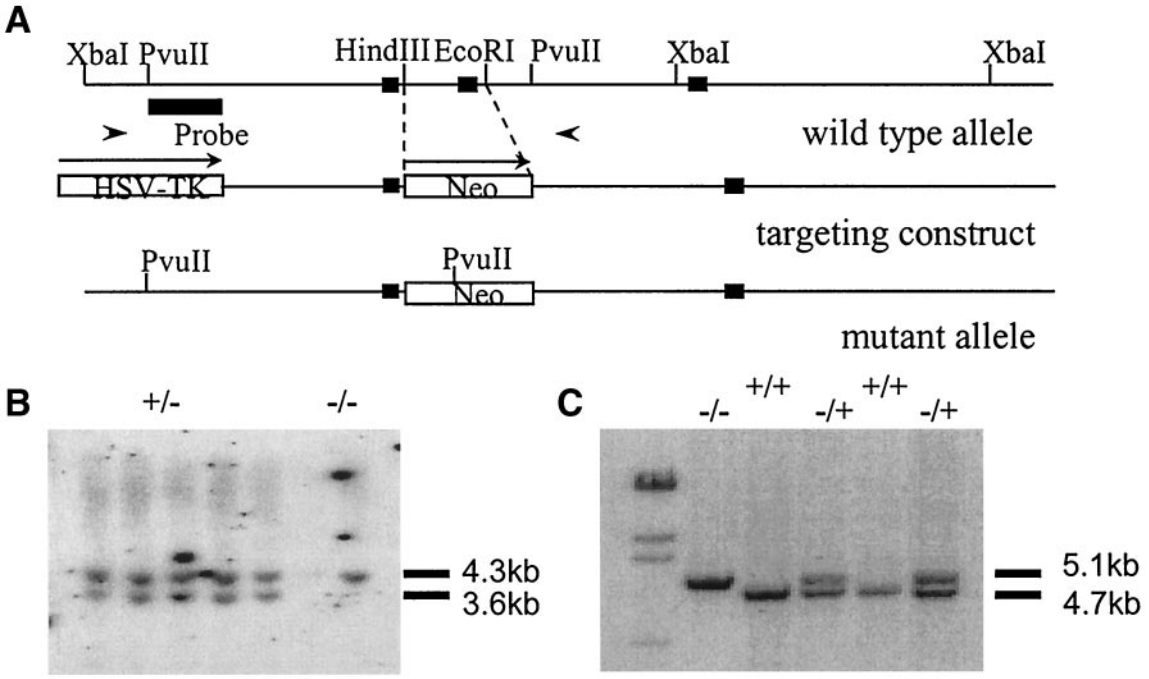

FIG. 1. Targeted disruption of the S100A9 locus. (A) Recombination strategy. A schematic representation of the S100A9 wild-type gene, the targeting construct, and the mutant allele are shown. Closed boxes represent the three exons of the S100A9 gene; the neomycin resistant gene (Neo) and thymidine kinase gene (HSV-TK) are indicated by open boxes. Arrows represent the direction of transcription. The region indicated as the probe was used for the screening of targeted ES cells. Arrowheads indicate PCR primers used for detection of the mutant allele. The predicted sizes of DNA fragments in Southern blot analysis and PCR are also shown. (B) Southern blot analysis of five selected ES cell clones. Genomic DNA was digested with *Pvu*II and hybridized with the probe shown in panel A. The observed 4.3- and 3.6-kb bands represent the wild-type and mutated alleles, respectively. (C) PCR analysis of tail DNAs from 4-week-old progeny. After PCR amplification of wild-type and targeted alleles, DNA fragments of 4.7 and 5.1 kb were detected.

mouse ER-MP20 (T-2004); from Serotec, Ltd., rat anti-mouse F4/80 (A3-1); from Dianova (Hamburg, Germany), peroxidase-conjugated goat anti-rabbit IgG, peroxidase-conjugated goat anti-rat IgG, and FITC-conjugated goat anti-rabbit IgG; and from Miltenyi Biotec (Bergisch-Gladbach, Germany), magnetic-bead-conjugated anti-CD11b. Our laboratory produced the rabbit polyclonal antibodies against mouse S100A8 and S100A9. Recombinant human IL-8 and leukotriene B_4 (LTB_4) were purchased from TEBU (Offenbach, Germany) and Sigma (Taufkirchen, Germany), respectively. IL-3, granulocyte-macrophage colony-stimulating factor (GM-CSF), and granulocyte colony-stimulating factor (G-CSF) were ordered from R&D Systems (Wiesbaden, Germany).

Culture medium. Cell-culture-grade buffers (phosphate-buffered saline [PBS] without Ca^{2+} or Mg^{2+}, Hanks balanced salt solution [HBSS] with Ca^{2+} and Mg^{2+}), media (Dulbecco's modified Dagle's medium [DMEM], RPMI 1640, and Iscove's modified Dulbecco's medium [IMDM]), antibiotics, and sera were purchased from Biochrom (Berlin, Germany).

Targeting construct. The targeting vector (Fig. 1) was constructed by replacing 760 bp of the genomic sequence containing exon 2 and the adjacent intron region with the pMC1-derived neomycin-poly(A) expression cassette (Stratagene, Amsterdam, The Netherlands). This mutation deletes the initial start codon. The resulting construct was linearized with *Not*I and electroporated into the embryonic stem (ES) cell line E14-1-1 (13) derived from 129/Ola mice. Resistant colonies were isolated following selection in G418 and ganciclovir and expanded as described previously (9).

Generation of S100A9-deficient mice. Cells of four independent ES clones were microinjected into the blastocysts of C57BL/6 mice. Chimeras were bred against the background of the host blastocyst. Heterozygote mice carrying the S100A9 mutation were interbred, and the offspring were genotyped by PCR. Both the $S100A9^{+/+}$ (wild-type) and S100A9-deficient animals were bred under specific pathogen-free conditions and studied from 6 to 20 weeks of age.

To analyze the offspring, PCR from tail DNA was performed using the following primers: upstream, 5′-CTCGGTCAAATGTGCCTAAC, and downstream, 5′-GTCTTTAACCAGGGACTAGG. PCR was performed with a thermal cycler for 10 cycles at 94°C for 90 s, 55°C for 120 s, and 72°C for 390 s, followed by 30 cycles at 94°C for 90 s, 55°C for 80 s, and 72°C for 390 s. Final extension was done at 72°C for 600 s. After PCR amplification of wild-type and targeted alleles, DNA fragments of 4.7 and 5.1 kb were detected.

Isolation of leukocytes. Mouse bone marrow cells were flushed from femurs and tibias with PBS. Erythrocytes were lysed with lysis buffer (155 mM NH_4Cl, 10 mM $KHCO_3$, 0.1 mM EDTA) for 4 min at room temperature, and the remaining cells were washed once with PBS. Polymorphonuclear neutrophils (PMNs) were isolated by magnetic cell separation using CD11b microbeads (Miltenyi Biotec) according to the manufacturer's instructions. Peripheral leukocytes were purified from heparinized blood from axillary vessels. Neutrophils were analyzed by flow cytometry after specific immunostaining. Thioglycolate-elicited PMNs were harvested as described below.

RNA isolation and detection. Total RNA was isolated from blood, spleen, liver, brain, and thioglycolate-elicited PMNs by using a commercially available reagent (peqGOLD TriFast; peqlab Biotechnologie GmbH, Erlangen, Germany) according to the manufacturer's instructions. Northern blot analysis was performed according to standard procedures. Briefly, total RNA was loaded on a 1% agarose–2.2 M formaldehyde denaturing gel and transferred to a nylon membrane (Hybond; Amersham Bioscience Europe, Freiburg, Germany). Blots were hybridized with ^{32}P-labeled cDNA probes (performed with the HexaLabelDNA labeling kit; MBI Fermentas, St. Leon-Rot, Germany). Total RNA was also reverse transcribed into cDNA with Moloney murine leukemia virus-Superscript II polymerase following the recommendations of the supplier (Gibco BRL via Invitrogen, Karlsruhe, Germany) by using an $oligo(dT)_{12\text{-}18}$ primer (MWG-Biotech, Munich, Germany). Amplification of cDNA was performed with TaKaRa Ex *Taq* DNA polymerase (BioWhittaker, Verviers, Belgium) and specific oligonucleotides for S100A8 (sense, 5′-GAAATCACCATGCCCTCTAC; antisense, 5′-CCCACTTTTATCACCATCGC), and S100A9 (sense, 5′-CTCTAGGAAGGAAGGACACC; antisense, 5′-GCCATCAGCATCATACACTC). The reaction conditions included 30 cycles of amplification at 94, 55, and 72°C for 90, 120, and 120 s, respectively. Final extension was done at 72°C for 600 s.

Flow cytometric analysis. Immunofluorescence staining was performed after washing the cells once with PBS–0.5% bovine serum albumin (BSA). Cells (10^6)

were first incubated with each anti-MAb (5 μg/ml) diluted in PBS-BSA for 30 min on ice. After three washes with PBS, cells were incubated with FITC- and phycoerythrin-conjugated second-step antibody for 30 min on ice. After washing twice with PBS, the cells were analyzed by flow cytometry with FACStar (Becton Dickinson). For the detection of S100A8 and S100A9, fixation and permeabilization were performed in acetone before intracellular staining.

Immunohistochemistry. Cryostat sections (5 to 8 μm thick) and cytospin preparations were fixed in acetone for 10 min at room temperature and washed in PBS. Endogenous peroxidase activity was blocked by incubating the preparations in sodium azide (Sigma) diluted at 1g/150 ml of PBS plus 0.035% H_2O_2 for 20 min at room temperature. PBS–1% BSA was used to block nonspecific binding for 60 min. Preparations were stained with primary antibody, followed by incubation with peroxidase-conjugated goat anti-rat or anti-rabbit IgG in PBS–1% BSA–20% inactivated mouse serum for 60 min. Enzymatic color development was performed by using 3-amino-9-ethylcarbazole (Sigma) as substrate, which was diluted in acetate buffer with 0.014% H_2O_2 at 37°C for 12 min. Slides were then counterstained with Giemsa stain and mounted with Aquamount mounting medium (BD PharMingen).

Colony-forming assay. Bone marrow cells were held in IMDM with antibiotics and 20% fetal calf serum (FCS). One hundred thousand cells were seeded into one well of a six-well dish in 1 ml of medium containing 0.35% low-melting-point agarose (SeaPlaque; Biozyme) and 20 ng of the indicated cytokine. After 10 days of incubation, colonies were counted (bone marrow cell numbers per colony were >50 for cells from S100A9-deficient mice versus >20 for cells from wild-type mice which responded to G-CSF).

PMN emigration into the skin and peritoneum. IL-8 (40 ng in 8 μl of PBS) or PBS was injected subcutaneously into both ears of the mice. Four hours after injection, the skin at the injection site was excised, embedded, frozen in N_2, sectioned at an 8-μm thickness, fixed in acetone, and stained in two steps with rat anti-mouse Ly-6G (Gr1) and a peroxidase-conjugated anti-rat IgG antibody (Fig. 12). To evaluate emigration, the Gr1-positive cells were counted in five fields of vision in five sections per ear. Five mice of both the S100A9-deficient and wild-type genotypes were used for the experiment.

Thioglycolate-elicited PMNs were harvested from the peritoneum at various time points after intraperitoneal injection of 1 ml of thioglycolate (3% [wt/vol] in PBS) by subjecting to lavage with 5 ml of PBS containing 2 mM EDTA. Total numbers of emigrated cells were counted with a Neubauer hemocytometer. Leukocyte subpopulations were determined by cytological examination of antibody-stained cytospin preparations.

TEM. Transendothelial migration (TEM) was determined by using a chemotaxis microchamber (Transwells, 5-μm pore size; Corning). Bone marrow cells were suspended at 2×10^6 cells/ml in DMEM supplemented with 10% FCS. One hundred microliters of cell suspension was applied to the upper chamber on a monolayer of bEnd5 cells (2×10^4/200 μl of DMEM, 10% FCS; day 3). Cytokines, IL-8 (1 μg/ml), and LTB_4 (25 nmol) were added to the lower chamber. After incubation at 37°C for 2 h, cells that migrated to the lower chamber were collected and counted with Coulter (Krefeld, Germany) Counter Z2. Cytospin preparations of the migrated cells were then immunocytochemically stained to determine the proportions of the cell subpopulations.

Measurement of cell migration within a 3-D collagen matrix. Cell migration within a three-dimensional (3-D) collagen matrix was studied as described previously (7, 8). Five hundred thousand neutrophils (isolated from the peritoneal cavity 4 h after the induction of peritonitis) were suspended in 20 μl of medium (RPMI plus 10% FCS) and added to 40 μl of a solution containing dermal bovine collagen type I (Nutacon, Leimuiden, The Netherlands). The final concentration for collagen was 1.6 mg/ml. This suspension was used to fill a self-constructed chamber consisting of a basal microscope slide and an upper coverslip sealed on three sides with paraffin and petroleum jelly at a ratio of 1:1. After polymerization (37°C, 5% CO_2, 20 to 30 min), the chamber was filled with medium and basal cell migration was recorded by time lapse video microscopy for 2 h. Replacing the medium with fresh medium containing 500 ng of IL-8/ml stimulated thereafter the locomotion of cells. Cell migration was then further documented over a period of 1 day. Subsequently, the paths of 40 individual cells were reconstructed from the recorded films for a period of up to 4 h by computer-assisted cell tracking (8). For data analysis, 40 cells of each sample were randomly selected. Subsequently, the movements of each of these cells were individually followed with a trackball over a period of 90 min. Every 2 min, the x and y coordinates of the screen pointer were registered by the computer. Plotting these x and y data on the screen reconstructed the path of each cell. From the obtained migration data, velocity (excluding migration breaks) and migration distance were calculated for each cell and the mean for all 40 cells was taken.

Actin polymerization. Bone marrow cells were resuspended in PBS at a concentration of 5×10^7 cells/ml, preincubated for 5 min at 37°C, and exposed to IL-8 for various times. The cells were then fixed with 3.7% paraformaldehyde–PBS for 30 min at room temperature and rinsed in buffer containing 0.2% gelatin and 0.01% Triton X-100. Cells were then incubated for 45 min in the dark with 5 μg of fluorescein-phalloidin (Sigma)/ml diluted in PBS. After washing and resuspension in PBS, the fluorescence of gated Gr1-positive cells was measured by flow cytometry.

The intracellular F-actin distribution was visually verified by fluorescence microscopy. CD11b-positive cells purified from bone marrow (10^6) were resuspended in PBS, incubated with or without IL-8 (250 ng/ml) for 30 s at 37°C, loaded into the chamber of a slide (LAB-TEK; Nalge Nunc International) containing a solution of 5% paraformaldehyde–PBS, and sedimented for 30 min at room temperature. Supernatant was removed, and FITC-phalloidin staining was performed as described above. Cell preparations were mounted with fluorescent mounting medium (DAKO) and observed with a fluorescence microscope, and representative cells were photographed.

CD11b expression. Bone marrow cells were prewarmed in either PBS (without Ca^{2+} or Mg^{2+}) or HBSS (with Ca^{2+} and Mg^{2+}) plus 0.1% BSA for 5 min and then incubated with various concentrations of IL-8 for 5 min and 30 min at 37°C. After incubation, the expression levels of CD11b were determined by flow cytometry with anti-CD11b antibody.

Adhesion assay. bEnd5 cells were plated at a density of 10^5 cells per well in 96-well plates 2 days prior to the test. Bone marrow cells (5×10^4 in 0.1 ml of HEPES) were added to confluent bEnd5 cells pretreated with tumor necrosis factor alpha (TNF-α) (100 ng/ml, 2 h) and allowed to adhere for 20 min at 37°C. IL-8 was added to a final concentration of 400 ng/ml where indicated. After incubation, plates were washed three times with HEPES buffer. Fifty microliters of 0.5% hexadecyltrimethylammonium bromide (Sigma) was added to each well for 30 min to lyse the cells. Myeloperoxidase activity was used as a marker enzyme to measure the number of leukocytes that adhered as described previously. Briefly, the optical density at 450 nm was measured after 15 min of incubation with 250 μl of 0.2 mg of dianisidine dihydrochloride (Sigma)/ml–0.4 M H_2O_2 in PBS.

RESULTS

S100A9-deficient mice appear to be healthy and develop normally. Two genomic clones encompassing the entire coding region of the murine S100A9 gene were isolated and characterized (20). We replaced the second exon, which includes the translational start site, with the neomycin cassette by using homologous recombination (Fig. 1). Chimeric mice were generated from four independent targeted ES cell clones. Wild-type, homozygous mutant, and heterozygous (+/−) mice were born with expected Mendelian frequencies, indicating that the mutation did not affect their survival in utero. At birth, all littermates were indistinguishable. Adult S100A9-deficient mice were viable and fertile and showed no abnormality. Homozygous mice derived from the four ES cell clones were indistinguishable with respect to growth and weight. Northern blotting and reverse transcription (RT)-PCR analysis confirmed the absence of S100A9 RNA transcripts in various organs of the deficient mice (Fig. 2C and D). The absence of S100A9 in the blood and bone marrow cells was demonstrated by flow cytometric analysis and Western blot experiments (Fig. 2A) and immunostaining of cytospin preparations with a polyclonal anti-mouse S100A9 antibody (Fig. 3). Histological analysis of the brain, thymus, heart, lung, liver, kidney, spleen, lymph nodes, small and large intestines, and skin from wild-type and S100A9-deficient mice revealed no morphological alterations. The cell number, shape, and anatomy of various organs of the S100A9-deficient mice appeared to be normal (data not shown).

Deficiency of S100A9 does not affect the number and morphology of peripheral leukocytes. The number and morphology of leukocytes in the peripheral blood of mutant and wild-type mice were normal. To further determine whether the loss

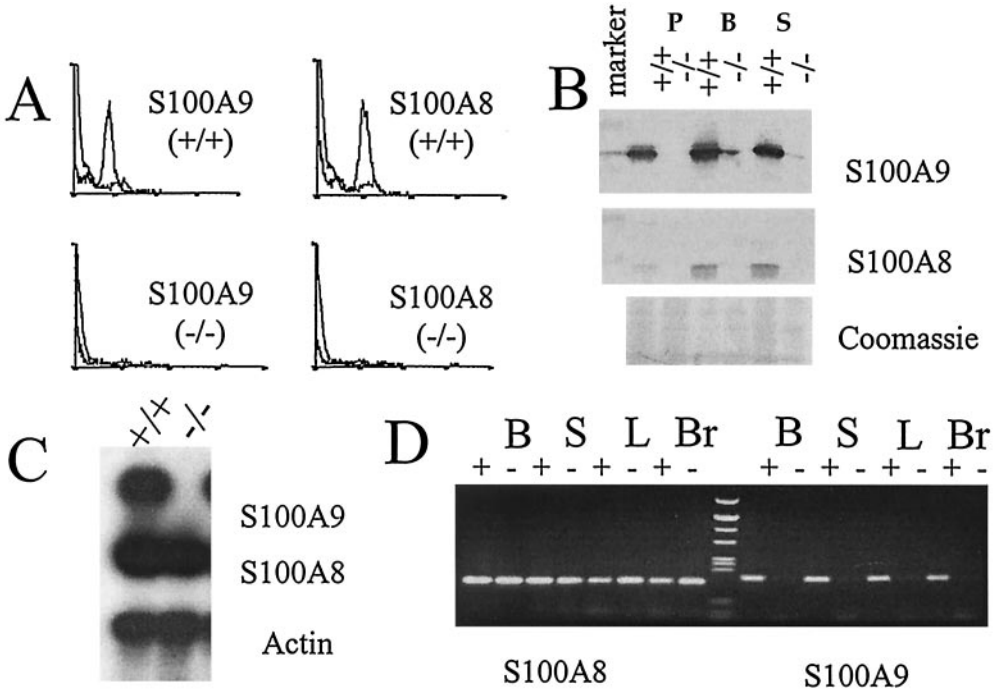

FIG. 2. Expression of S100A8 in mice lacking a functional S100A9 gene. (A) Flow cytometric profiles after S100A9 and S100A8 immunostaining of blood neutrophils are shown. Profiles are representative of three mice for each genotype. Analysis reveals the absence of both proteins in peripheral blood cells. (B) Western blot analysis of S100A9 and S100A8 expression in wild-type and S100A9-deficient mice demonstrates the absence of S100A9 and S100A8 in peripheral S100A9-deficient leukocytes. The upper part of the S100A8 filter was stained with Coomassie brilliant blue to confirm the transfer of the proteins to the filter. P, peritoneal granulocytes; B, bone marrow; S, spleen. (C) Northern blot analysis demonstrates the absence of S100A9 mRNA in thioglycolate-elicited peritoneal PMNs from S100A9-deficient mice, whereas the S100A8 gene is transcribed in wild-type as well as S100A9-deficient cells. Signals presented are shown as gene expression relative to the average expression of the housekeeping gene actin. (D) RT-PCR analysis confirms the absence of S100A9 RNA transcripts in various organs of deficient mice (right panel) and shows the presence of S100A8 RNA transcripts in the same organs (left panel). B, brain; S, spleen; L, liver; Br, brain.

of S100A9 protein affects the differentiation of myeloid cells, we examined the expression of various specific cell markers in bone marrow cells daily during the 4 days of cultivation. Immunostaining of cytospin preparations with the specific cell markers CD11b, Gr1, ERMP12, and ERMP20 (Fig. 4) demonstrated a slight reduction of the indicated cell subpopulations in S100A9-deficient mice. The number of Gr1-positive cells especially, mainly granulocytes, was reduced in S100A9-deficient bone marrow. The numbers of B220 and Thy-1.2 lymphocytes were equal (data not shown).

To further evaluate the myelopoietic potential, we performed colony-forming assays. Here, stimulation of bone-marrow-derived cells from S100A9-deficient mice with IL-3 resulted in a reduced number of colonies (more than 50 cells per colony). However, a large number of small colonies with fewer than 50 cells were observed (data not shown). Furthermore, more of the S100A9-deficient cells than of the wild-type bone marrow cells responded to G-CSF or macrophage colony-stimulating factor (M-CSF), which supports the growth of more mature cells of the myeloid lineage (Fig. 5). Thus, we observed a shift to more mature myeloid precursor cells in S100A9-deficient bone marrow.

Loss of both S100A9 and S100A8 seems to be compatible with viable and mature granulocytes. Among the various tertiary structures S100A9 can adopt, the heterodimer with S100A8 is strongly preferred. Consequently, we studied the expression of S100A8 in detail. The S100A9 deficiency resulted in a 30% reduction of S100A8-positive cells in the bone marrow (Fig. 3 and 4), and this value drastically decreased during cultivation of the cells (~60% reduction on day 2 of culture). However, under inflammatory conditions, the number of S100A8-positive cells in the bone marrow of S100A9-deficient mice was similar to that of the wild-type mice (see Fig. 12B). To investigate the S100A8 expression in peripheral cells, flow cytometric analysis of blood cells (Fig. 2A) and immunostaining of the cytospin preparations of thioglycolate-elicited peritoneal PMNs and the cryosections of spleens (Fig. 3) from S100A9-deficient mice was conducted. These experiments as well as Western blot experiments (Fig. 2B) failed to detect S100A8, indicating that, in peripheral mature S100A9-null cells, the S100A8 protein is either absent or at least not detectable with our antibody. However, Northern blotting and RT-PCR analysis (Fig. 2C and D) showed the presence of the S100A8 mRNA transcripts in various organs from S100A9-deficient mice, suggesting that the strong down-regulation of S100A8 protein relies upon a posttranscriptional mechanism.

TEM in vitro is altered. To investigate the migratory properties of deficient neutrophils quantitatively, we performed in vitro assays to determine the TEM of bone-marrow-derived cells (Fig. 6). During 2 h of incubation, 3% of wild-type cells spontaneously migrated across an unstimulated bEnd5 mono-

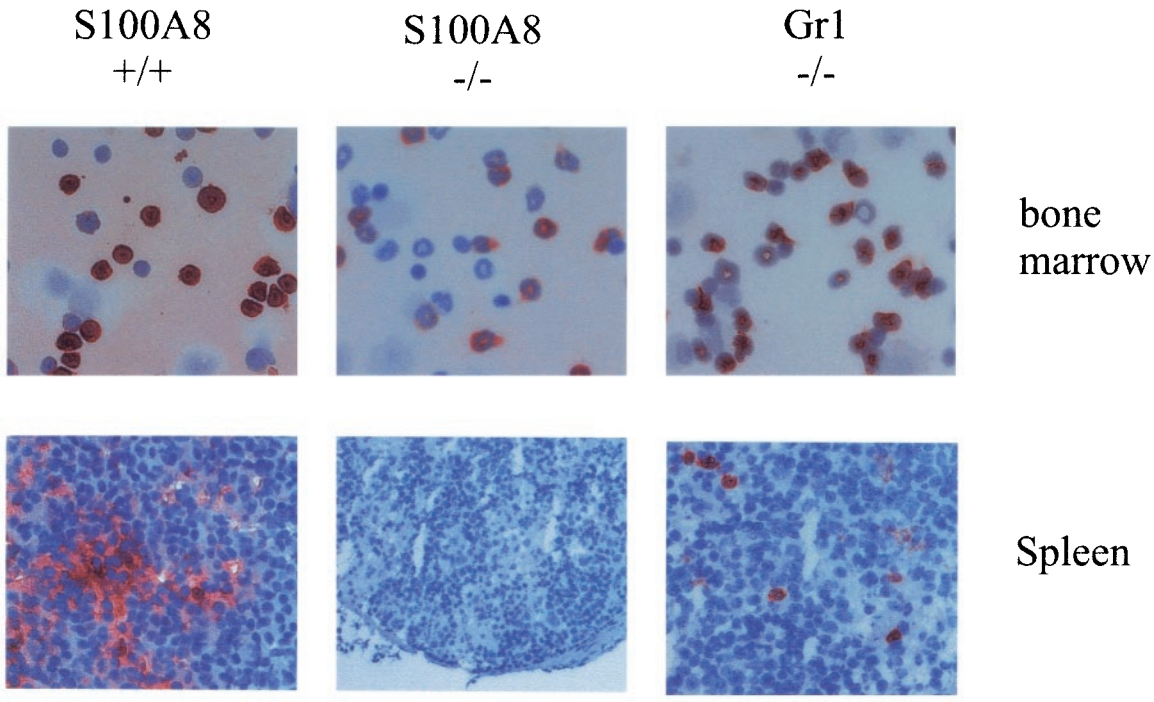

FIG. 3. Expression of S100A8 in S100A9-deficient bone marrow and spleen cells. As indicated, spleen and bone marrow cells were stained with the S100A8 antibody. As a control, granulocytes were stained with a commercially available gr1 antibody. S100A8 is present in bone marrow but not detectable in the peripheral tissues of the spleen.

layer. Surprisingly, the S100A9-deficient cells (13.5%) displayed a higher spontaneous migration activity in this assay. The percentage of cells that migrated was calculated by dividing the number of cells found in the lower well by the total number of cells added on top of the bEnd5 monolayer in the upper well.

IL-8 and LTB_4 attract preferentially neutrophils and monocytes, as judged by microscopic observation of the immunostained cytospin preparations of migrated cells. The majority of cells (95 to 100% unstimulated, IL-8 or LTB_4 stimulated) from wild-type and S100A9-deficient mice were positively stained with anti-mouse Gr1 antibody, confirming that, almost exclusively, granulocytes were migrating under the conditions used. Approximately 100% of the IL-8- and 86% of the LTB_4-

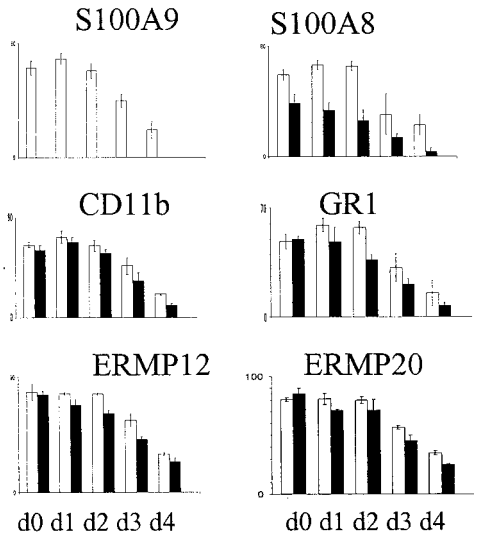

FIG. 4. Analysis of the hematopoietic cell population. Bone marrow from wild-type and S100A9-deficient mice were cultured for 4 days (d) in Teflon bags and analyzed daily by immunostaining of cytospin preparations for the expression of indicated cell markers in order to follow the differentiation of myeloid cells. Bars presented are the means from five separate experiments. In all panels, white bars correspond to wild-type mice and black bars correspond to S100A9-deficient mice.

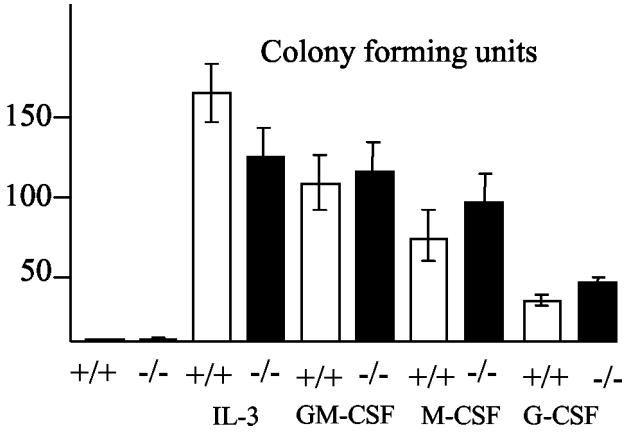

FIG. 5. CFU experiments using wild-type and S100A9-deficient bone marrow leukocytes. Bone marrow cells from wild-type and S100A9-deficient mice were incubated with the cytokines indicated to evaluate the myelopoietic potential of the precursor cells. As a control, bone marrow cells were incubated without any cytokines.

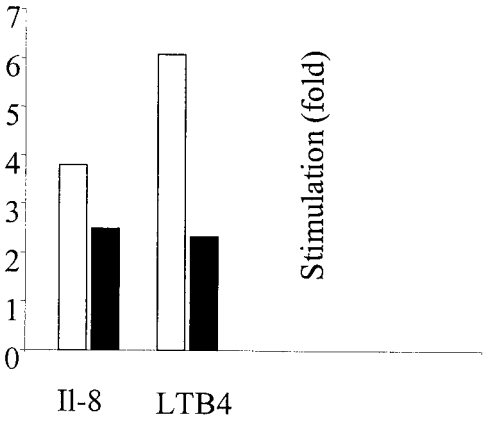

FIG. 6. Chemoattractant-induced in vitro TEM assay. TEM of bone marrow cells from wild-type (white bars) and S100A9-deficient (black bars) mice through a bEnd5 monolayer is shown. Values represent the means from four experiments. The stimulation rate was calculated by dividing the number of transmigrated cells after stimulation by the number before stimulation. Values are means ± standard errors of the means and were considered significant at a P of <0.01.

stimulated wild-type cells were stained with anti-mouse S100A8 antibody. IL-8 and LTB_4 increased the TEM of wild-type neutrophils 3.8- and 6.1-fold. The TEM values for S100A9-deficient neutrophils were stimulated only 2.5- and 2.3-fold, respectively (Fig. 6).

Chemokinesis of S100A9-deficient neutrophils in a 3-D collagen matrix. To further characterize the migratory properties of S100A9-negative neutrophils, we measured various dynamic parameters (cell velocity, migration rate, and migration distance) within a 3-D collagen matrix in the absence or presence of additional external stimuli. The increased spontaneous activity of S100A9-deficient neutrophils observed in TEM could not be confirmed in the 3-D collagen matrix assay (Fig. 7). The migration distance and the number of simultaneously migrating cells, as well as the velocity of $S100A9^{-/-}$ and $S100A9^{+/+}$ neutrophils, were similar. Stimulation of the cells with IL-8 was accompanied by significant changes in the dynamic parameters (Fig. 7). The migration rate of wild-type cells was slightly higher than that of the S100A9-deficient cells. This increase could be due to both the recruitment of previously nonmigrating cells and the increased duration of migration. Additionally, wild-type cells were able to cover greater distances than S100A9-deficient cells (~70 and ~50 μm, respectively). Cell velocity of wild-type peritoneal neutrophils was also higher than that of deficient neutrophils after stimulation with IL-8. The differences were significant according to statistical evaluation ($P < 0.05$).

CD11b surface expression is disturbed in neutrophils from S100A9-deficient mice. CD11b belongs to the integrin family of proteins. It has been reported that S100A9 is involved in the expression and modulation of CD11b (5, 19). CD11b cell surface expression was reduced on the surface of S100A9-deficient neutrophils (Fig. 8, lower panel) incubated in PBS. IL-8-induced CD11b up-regulation depends on the presence of Ca^{2+} and Mg^{2+}. Consequently, IL-8 failed to enhance CD11b surface expression in wild-type neutrophils by using Ca^{2+}- and Mg^{2+}-free buffers as expected. However, neutrophils from S100A9-deficient mice exhibited an initial decrease in CD11b expression at concentrations below 200 ng of IL-8/ml under calcium-free conditions (Fig. 8).

Incubation of cells in calcium containing HBSS buffer restores CD11b surface expression. Incubation of bone-marrow-derived neutrophils from wild-type mice with various concentrations of IL-8 in HBSS (containing Ca^{2+} and Mg^{2+}) for 5 min at 37°C induced a 1.7-fold increase in the membrane expression of CD11b on Gr1-gated cells as measured by flow cytometry (Fig. 8, upper panel). A maximal increase was achieved at 250 ng of IL-8/ml. A higher concentration (750 ng/ml) did not further potentiate the up-regulation. In contrast, S100A9-null neutrophils failed to up-regulate the cell surface expression of CD11b upon IL-8 stimulation.

IL-8 may not be able to enhance adhesion of S100A9-deficient neutrophils to bEnd5 endothelial cells. As reported earlier (3, 10, 24), IL-8 stimulates neutrophils to adhere to endothelial cells by an up-regulation of β2 integrin CD11b surface expression. Therefore, we analyzed the adhesion of S100A9-

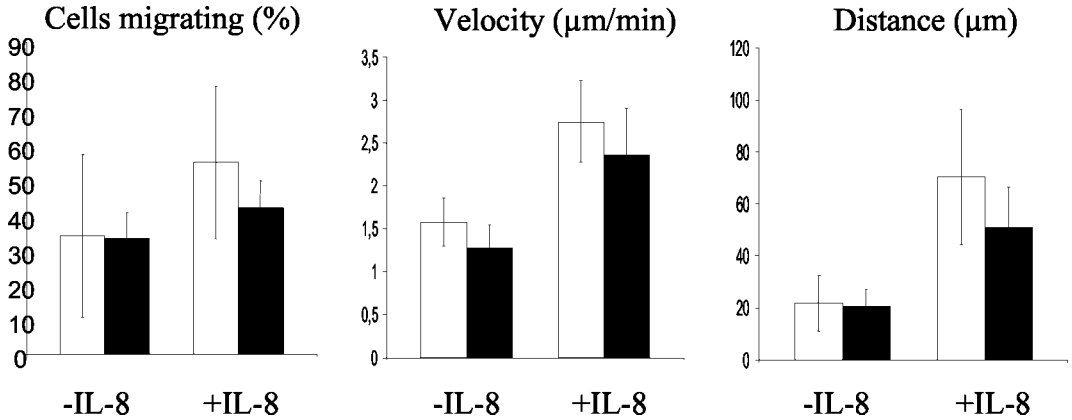

FIG. 7. Dynamic parameters of spontaneous and chemokine-induced migration of S100A9-deficient and wild-type peritoneal neutrophils. The data show the means from four independent experiments. In all panels, white bars correspond to wild-type neutrophils and black bars correspond to S100A9-deficient neutrophils. All parameters indicate a reduced chemokinesis of the S100A9-deficient neutrophils upon stimulation with IL-8. Values were considered significant at a P of <0.05.

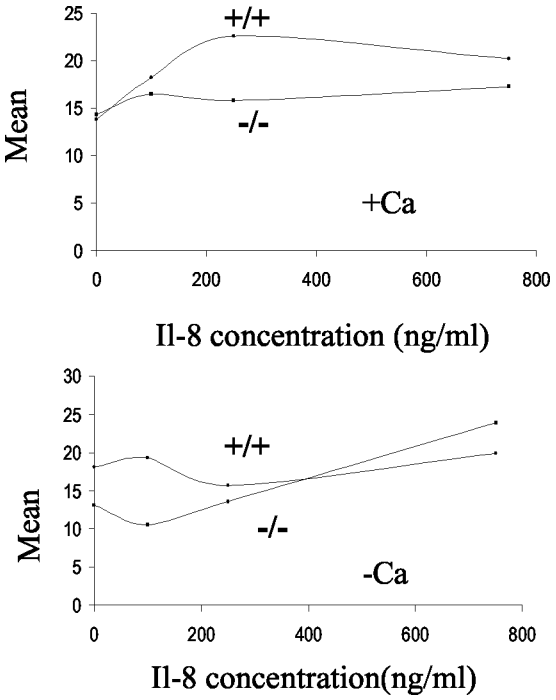

FIG. 8. IL-8-mediated surface expression of CD11b on Gr1-gated cells. Bone marrow cells were incubated at 37°C for 5 min with or without IL-8 and in the presence (upper panel) or absence (lower panel) of Ca^{2+} and Mg^{2+}. At the end of the incubation period, surface expression of CD11b on Gr1-gated cells was determined by direct-immunofluorescence flow cytometry. The data presented here show one experiment representative of five experiments.

deficient neutrophils to bEnd5 endothelial cells. No IL-8-dependent increase of adhesion of S100A9-deficient cells could be detected, whereas IL-8 stimulation of wild-type neutrophils enhanced adhesion to TNF-α-activated bEnd5 cells (Fig. 9). However, statistically, the difference seems to not be significant. The number of adherent cells did not differ when mutant

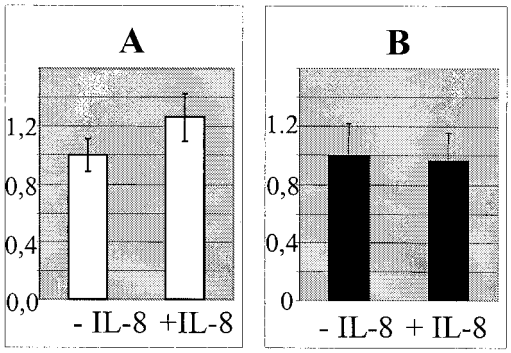

FIG. 9. IL-8 failed to enhance the adhesion of S100A9-deficient neutrophils to bEnd5 cells. bEnd5 cells were incubated with TNF-α for 2 h; subsequently, $S100A9^{-/-}$ (B) and wild-type (A) leukocytes were allowed to adhere for 1 h with or without IL-8. After washing, the myeloperoxidase activity was determined to measure the number of neutrophils that adhered. To compare the unstimulated and IL-8-stimulated conditions, the value obtained for the unstimulated neutrophils was set to 1.0.

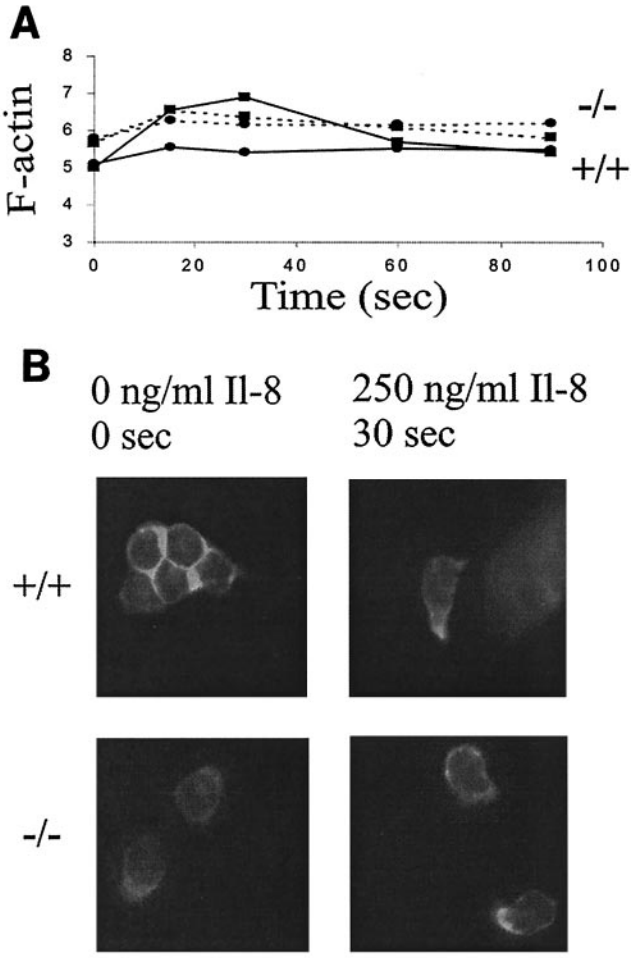

FIG. 10. F-actin content in unstimulated S100A9-deficient PMNs is higher than that in wild-type PMNs. (A) The time course of IL-8-induced changes in the cellular F-actin content in Gr1-gated cells is shown. Broken lines represent data for $S100A9^{+/+}$ mice, and dotted lines represent data for $S100A9^{-/-}$ mice. Levels of IL-8 are either 0 ng/ml (circle) or 250 ng/ml (square). The values represent the means from five separate experiments. (B) The photographs show the F-actin distribution in unstimulated (left panels) and IL-8-stimulated (right panels) $CD11b^{+}$ cells isolated from bone marrow.

and wild-type neutrophils were not stimulated with IL-8 (data not shown).

G- to F-actin shift in nonstimulated S100A9-deficient PMNs suggests a role of S100A9 in cytoskeletal reorganization. Chemotaxis is critically dependent on cytoskeletal dynamics (10), and actin is considered the most important cytoskeletal element for migration. Thus, the ability of IL-8 to induce actin polymerization was investigated in S100A9-deficient PMNs. Fluorescence emission of single cells after FITC-phalloidin staining was recorded as a measure of the F-actin content of individual PMN. Immediately after the addition of 250 ng of IL-8/ml, an increase of F-actin content in wild-type PMNs was observed (Fig. 10A). The maximum increase was 1.27-fold at 30 s. In contrast, almost no increase in F-actin content was seen in S100A9-deficient PMNs. Instead, a difference in the average mean fluorescence of nontreated wild-type versus S100A9-deficient cells was observed, indicating that F-actin content was

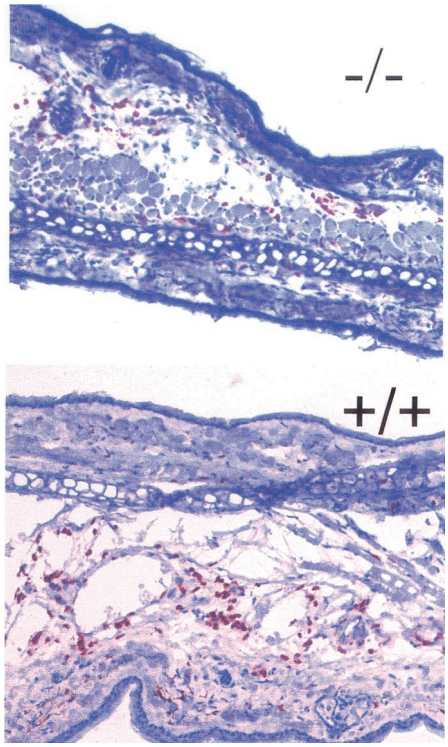

FIG. 11. IL-8-induced emigration of neutrophils into the skin. IL-8 was injected into the ears of wild-type and S100A9-deficient mice. The number of Gr1-stained cells 4 h after IL-8 injection was visually evaluated. There was no difference observed between the number of emigrated neutrophils with respect to the wild-type and S100A9-deficient mice.

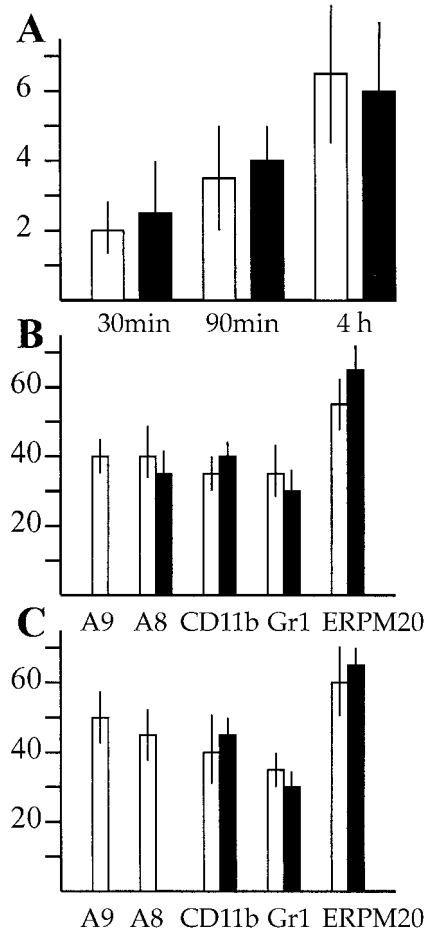

FIG. 12. Thioglycolate-elicited leukocyte emigration into the peritoneum. (A) The total number of leukocytes migrated into the peritoneum subsequent to intraperitoneal injection of thioglycolate was determined at various time points as indicated (10^6). No significant difference was observed between S100A9-deficient (black bars) and wild-type (white bars) mice. Each bar represents the mean values for at least 10 mice. (B) Cellular composition of bone marrow cells was analyzed subsequent to thioglycolate-induced peritonitis (4 h). After inflammatory stimulation of the granulopoiesis, the percentage of S100A8-positive cells in the bone marrow was similar in wild-type and S100A9-deficient mice. (C) Cellular composition (percentage of positive cells) of the peritoneal exudate was determined cytochemically with various cellular surface markers as indicated. No deviation was observed between S100A9-deficient and wild-type mice.

higher in unstimulated deficient PMNs than in unstimulated wild-type PMNs. We could not observe a subsequent decrease in the F-actin content. Additionally, cell morphology and F-actin distribution were investigated by conventional fluorescence microscopy. Prior to stimulation, wild-type PMNs were round, with fluorescence homogeneously distributed in the cytoplasm (Fig. 10B). They underwent a polarization change of shape 30 s after stimulation with 250 ng of IL-8/ml, and fluorescence was localized in one pole or in developing pseudopods. S100A9-deficient PMNs appeared polarized without stimulation. Intracellular F-actin localization was similar to that of polarized wild-type PMNs after IL-8 stimulation. In conclusion, unstimulated S100A9-deficient PMNs showed an abnormal polarized cell shape with accumulation of F-actin in pseudopods, suggesting a role of S100A9 in cell morphology and cytoskeletal regulation.

PMN emigration into the tissue is normal, applying two in vivo models. The cytokine IL-8 (40 ng or buffer alone) was injected into the ear. PMN recruitment was assessed by immunostaining of cryostat sections with anti-mouse Gr1 antibody (Fig. 11). Histological examination of the preparations revealed that the subcutaneous injection of IL-8 provoked a similar PMN infiltration in wild-type and deficient mice.

We measured the emigration of leukocytes of thioglycolate-elicited peritoneal PMNs. Various time points after the injection of thioglycolate, total numbers of peritoneal exudate cells were determined by microscopic observation of tryptan blue-stained cells with a Neubauer hemocytometer. There was no significant difference between the number of cells emigrated into the peritonea of wild-type and S100A9-deficient mice (Fig. 12A). Immunostaining of cytospin preparations with anti-mouse MAbs (Gr1, CD11b, and ER-MP20) confirmed the recruitment of similar subpopulations of apparently mature PMNs; PMN purity was 75 to 85% 4 h after thioglycolate injection for deficient and wild-type mice preparations, respectively.

DISCUSSION

The family of calcium-binding S100 proteins consists of 13 members that are tissue specifically expressed and whose func-

tions are poorly understood (5). Two members, S100A9 and S100A8, are almost exclusively expressed in myeloid cells and have long been known as inflammatory marker proteins. We generated S100A9-deficient mice to study the function of this molecule.

The S100A9-deficient mice were viable and appear to be healthy. This is in sharp contrast to S100A8-deficient animals. The S100A8-deficient embryos were resorbed by day 9.5 in the uterus. This may indicate an unexpected function of S100A8 in early embryogenesis (22). S100A9 is obviously dispensable for this function. The energetically favored heterodimerization of S100A8 and S100A9 and their almost identical expression pattern leads to the assumption that the heterodimers are the biologically active molecules. The difference in the viability of both mouse models suggests that both molecules bear biological functions independent of heterodimerization.

Furthermore, the peripheral S100A9-null leukocytes lack detectable amounts of S100A8. Thus, even the lack of both S100A8 and S100A9 comprising nearly 40% of the cytosolic proteins in wild-type neutrophils does not affect the development of viable and mature neutrophils. Moreover, we could not detect an up-regulation of any other S100 protein (data not shown). However, it is important to note that S100A8 transcription is not altered in the S100A9-deficient mice and that residual S100A8 below the detection limit may be present in peripheral S100A9-deficient neutrophils.

S100A8 is present in bone marrow cells. Our observation that the percentage of S100A8-positive cells in the bone marrow of S100A9-deficient mice increased after inflammatory stimulation of granulopoiesis suggests that S100A8 protein is expressed in early differentiation stages and may become unstable in mature granulocytes.

We investigated the myelopoietic potential in S100A9-deficient mice. The S100A9-deficient animals displayed a normal population of myeloid cells in the bone marrow, as shown by immunocytochemistry. It has been speculated in an earlier report that both S100 proteins may be involved in the terminal differentiation of myeloid cells by inhibiting casein kinase (18). Our results indicate that the deficiency of S100A9 is dispensable for myelopoiesis and mobilization. However, the reduced number of IL-3-responsive cells and the increased number of G-CSF- and M-CSF-induced colonies derived from the S100A9-deficient bone marrow allow speculation that a potential defect in early myelopoiesis may be compensated by an unknown mechanism.

The most prominent property of neutrophils is their ability to invade inflamed tissue. S100A9 and S100A8 have both been described as molecules involved in adhesion (22, 25, 30) and directed migration (14). The unusually high F-actin content in S100A9-deficient neutrophils functionally links S100A9 to cytoskeletal regulation. Actin filaments are the primary cytoskeletal elements mediating migration. A functional actin cytoskeleton is essential for the coordinated expression and cell surface exposition of integrins. Integrins are linked to actin filaments by a number of actin-binding proteins, and the integrin-dependent cell spreading of PMNs requires actin polymerization (2). The deregulated microfilament system may cause the abnormal induction of the CD11b surface expression observed in S100A9-deficient neutrophils. Numerous reports associate various S100 proteins with the regulation of cytoskeletal dynamics (5, 26, 32). S100A1 and S100B are supposed to be involved in microtubule metabolism. S100A1 additionally inhibits phosphorylation of the actin-capping molecule MARCKS. S100A10 is proposed to regulate the activity of annexin II, including its association with cytoskeleton constituents and its F-actin-bundling activity (5). Moreover, in striking similarity to our analysis, a more organized microfilament formation has also been shown in C6 glioma cells in which the expression of S100B has been selectively inhibited by antisense technology (28).

It has been reported that S100A8- and S100A9-positive cells express more CD11b than S100A8- and S100A9-negative monocytes (6) and belong to the first infiltrating cells in inflammatory lesions. The finding that the actin filament system is highly polarized in S100A9-deficient cells correlates with a reduced ability to migrate upon a stimulus, as shown in the 3-D collagen matrix migration assay. The failure to up-regulate CD11b may result in the absence of IL-8-mediated adhesion. IL-8 and LTB_4 (29) are known to up-regulate CD11b surface expression. The reduced ability of LTB_4 to stimulate the TEM of S100A9-deficient cells suggests that LTB_4 may also fail to enhance S100A9-deficient neutrophil adhesion. Consequently, both the disturbed microfilament system and the absence of chemoattractant-induced adhesion may be responsible for the strong attenuation of the chemotactic response, as observed with S100A9-deficient neutrophils in the TEM assay. The inability of S100A9-deficient cells to enhance CD11b surface expression upon stimulation weakens the potential of these cells to adhere and may thus explain the discrepancy between the diminished responsiveness to chemoattractants observed in the TEM assay and the less pronounced effect found in the collagen matrix assay. Furthermore, extracellular S100A9 is known to modulate the affinity of the CD11b integrin receptor (21) and may facilitate transmigration by contributing to the binding to endothelial heparan sulfate (25) and/or carboxylated proteoglycans (30), suggesting that reduced transmigration may additionally result from the lack of extracellular S100A9. However, applying two inflammatory models, we could not detect any significant difference in the leukocyte invasion in vivo by using S100A9-deficient mice. It is known that different inflammation models involve different inflammatory mediators and adhesion molecules. CD18-deficient mice unexpectedly show no inhibition of neutrophil emigration during sterile peritonitis by the intraperitoneal injection of thioglycolate and, on the contrary, even an increased emigration in other models (4, 17). Similarly, migration of PMNs in the thioglycolate peritonitis model is enhanced in mice lacking the tyrosine kinases Hck, FGr, and Lyn, known as members of the integrin-signaling pathway (16) as well as in CD11b-deficient mice (15). Obviously, there is more than one pathway orchestrating neutrophil emigration into inflamed tissue. The role of S100A9 and S100A8 may still prove to play a major role in in vivo inflammatory models other than those investigated here.

Most transduction pathways that induce cell migration involve components that regulate the intracellular calcium concentration. Calcium in turn acts on actin-associated proteins like MARCKS and gelsolin (29) and thereby regulates actin polymerization. The observation that firstly, the CD11b surface expression is reduced in calcium-free buffers in S100A9-defi-

cient cells, that secondly, extracellular calcium restores normal CD11b surface expression, and that the strictly calcium-dependent, IL-8-mediated up-regulation of CD11b cannot be observed in S100A9-deficient neutrophils suggests that primarily the calcium homeostasis of S100A9-deficient cells is affected. Alterations in Ca^{2+} homeostasis have also been reported in mice deficient in calbindin, S100B, and calretinin, all calcium-binding EF-hand proteins expressed in the cells of the central nervous system (1, 27, 33). Further investigations are in process to define the role of the S100A9 molecule in neutrophil's calcium metabolism.

Using gene-targeting technology, we demonstrated that loss of the massively expressed S100A9 protein results in a viable and obviously healthy mouse. However, we observed a dramatic posttranscriptional down-regulation of S100A8 protein. On the cellular level, S100A9-deficient neutrophils exhibited a more organized microfilament system and a reduction of IL-8 mediated CD11b surface up-regulation, resulting in a diminished potential to respond to chemoattractant molecules in vitro. Nonetheless, we could not detect any abnormal leukocyte emigration that applied two inflammatory in vivo models, suggesting that S100A8 and S100A9 molecules may be dispensable, at least for the inflammatory models investigated here.

ACKNOWLEDGMENTS

This project was generously supported by the SFB 293 project A10 (Deutsche Forschungsgemeinschaft).

The excellent technical assistance of D. Wiesmann, B. Küter-Luks, K. Fischer, and H. Hater is acknowledged. Many thanks to A. Kondrashov for his help with blastocyst injections. We also thank Claus Kerkhoff for critical reading of the manuscript.

REFERENCES

1. **Airaksinen, M. S., L. Eilers, O. Garaschuk, H. Thoenen, A. Konnerth, and M. Meyer.** 1994. Ataxia and altered dendritic calcium signaling in mice carrying a targeted null mutation of the calbindin D28k gene. Proc. Natl. Acad. Sci. USA **94:**1488–1493.
2. **Calderwood, D. A., S. J. Shattil, and M. H. Ginsberg.** 2000. Integrins and actin filaments: reciprocal regulation of cell adhesion and signaling. J. Biol. Chem. **275:**22607–22610.
3. **Detmers, P. A., S. K. Lo, E. Olsen-Egbert, A. Walz, M. Baggiolini, and Z. A. Cohn.** 1990. Neutrophil-activating protein 1/interleukin 8 stimulates the binding activity of the leukocyte adhesion receptor CD11b/CD18 on human neutrophils. J. Exp. Med. **171:**1155–1162.
4. **Doerschuk, C. M.** 2001. Mechanisms of leukocyte sequestration in inflamed lungs. Microcirculation **8:**71–88.
5. **Donato, R.** 2001. S100: a multigenic family of calcium-modulated proteins of the EF-hand type with intracellular and extracellular functional roles. Int. J. Biochem. Cell. Biol. **33:**637–668.
6. **Eue, I., C. Langer, A. Eckardstein, and C. Sorg.** 2000. Myeloid related protein (MRP-14) expressing monocytes infiltrate atherosclerotic lesions of ApoE null mice. Atherosclerosis **151:**593–597.
7. **Friedl, P., P. B. Noble, and K. S. Zanker.** 1993. Lymphocyte locomotion in three-dimensional collagen gels. Comparison of three quantitative methods for analysing cell trajectories. J. Immunol. Methods **165:**157–165.
8. **Gunzer, M., P. Friedl, B. Niggemann, E. Brocker, E. Kampgen, and K. S. Zanker.** 2000. Migration of dendritic cells within 3-D collagen lattices is dependent on tissue origin, state of maturation, and matrix structure and is maintained by proinflammatory cytokines. J. Leukoc. Biol. **67:**622–629.
9. **Hogan, B., R. Beddington, F. Costantini, and E. Lacy.** 1994. Manipulating the mouse embryo: a laboratory manual. Cold Spring Harbor Laboratory Press, Cold Spring Harbor, N.Y.
10. **Huber, A. R., S. L. Kunkel, R. F. Todd III, and S. J. Weiss.** 1991. Regulation of transendothelial neutrophil migration by endogenous interleukin-8. Science **254:**99–102.
11. **Jones, G. E.** 2000. Cellular signaling in macrophage migration and chemotaxis. J. Leukoc. Biol. **68:**593–602.
12. **Kerkhoff, C., I. Eue, and C. Sorg.** 1999. The regulatory role of MRP8 (S100A8) and MRP14 (S100A9) in the transendothelial migration of human leukocytes. Pathobiology **67:**230–232.
13. **Kühn, R., K. Rajewsky, and W. Muller.** 1991. Generation and analysis of interleukin-4 deficient mice. Science **254:**707–710.
14. **Lackmann, M., P. Rajasekariah, S. E. Iismaa, G. Jones, C. J. Cornish, S. Hu, R. J. Simpson, R. L. Moritz, and C. L. Geczy.** 1993. Identification of a chemotactic domain of the pro-inflammatory S100 protein CP-10. J. Immunol. **150:**2981–2991.
15. **Lowell, C. A., and G. Berton.** 1999. Integrin signal transduction in myeloid leukocytes. J. Leukoc. Biol. **65:**313–320.
16. **Meng, F., and C. A. Lowell.** 1998. A beta 1 integrin signaling pathway involving Src-family kinases, Cbl and PI-3 kinase is required for macrophage spreading and migration. EMBO J. **17:**4391–4403.
17. **Mizgerd, J. P., H. Kubo, G. J. Kutkoski, S. D. Bhagwan, K. Scharffetter-Kochanek, A. L. Beaudet, and C. M. Doerschuk.** 1997. Neutrophil emigration in the skin, lungs, and peritoneum: different requirements for CD11/CD18 revealed by CD18-deficient mice. J. Exp. Med. **186:**1357–1364.
18. **Murao, S., F. Collart, and E. Huberman.** 1990. A protein complex expressed during terminal differentiation of monomyelocytic cells is an inhibitor of cell growth. Cell Growth Differ. **1:**447–454.
19. **Nacken, W., C. Sopalla, C. Propper, C. Sorg, and C. Kerkhoff.** 2000. Biochemical characterization of the murine S100A9 (MRP14) protein suggests that it is functionally equivalent to its human counterpart despite its low degree of sequence homology. Eur. J. Biochem. **267:**560–565.
20. **Nacken, W., J. A. Lekstrom-Himes, C. Sorg, and M. P. Manitz.** 2001. Molecular analysis of the mouse S100A9 gene and evidence that the myeloid specific transcription factor C/EBPepsilon is not required for the regulation of the S100A9/A8 gene expression in neutrophils. J. Cell. Biochem. **80:**606–616.
21. **Newton, R. A., and N. Hogg.** 1998. The human S100 protein MRP-14 is a novel activator of the beta 2 integrin Mac-1 on neutrophils. J. Immunol. **160:**1427–1435.
22. **Passey, R. J., E. Williams, A. M. Lichanska, C. Wells, S. Hu, C. L. Geczy, M. H. Little, and D. A. Hume.** 1999. A null mutation in the inflammation-associated S100 protein S100A8 causes early resorption of the mouse embryo. J. Immunol. **163:**2209–2216.
23. **Raftery, M. J., Z. Yang, S. M. Valenzuela, and C. L. Geczy.** 2001. Novel intra- and inter-molecular sulfinamide bonds in S100A8 produced by hypochlorite oxidation. J. Biol. Chem. **276:**33393–33401.
24. **Roberts, P. J., A. R. Pizzey, A. Khwaja, J. E. Carver, A. R. Mire-Sluis, and D. C. Linch.** 1993. The effects of interleukin-8 on neutrophil fMetLeuPhe receptors, CD11b expression and metabolic activity, in comparison and combination with other cytokines. Br. J. Haematol. **84:**586–594.
25. **Robinson, M. J., P. Tessier, R. Poulson, and N. Hogg.** 2002. The S100 family heterodimer, MRP-8/14, binds with high affinity to heparin and heparan sulfate glycosaminoglycans on endothelial cells. J. Biol. Chem. **277:**3658–3665.
26. **Roth, J., F. Burwinkel, C. van den Bos, M. Goebeler, E. Vollmer, and C. Sorg.** 1993. MRP8 and MRP14, S-100-like proteins associated with myeloid differentiation, are translocated to plasma membrane and intermediate filaments in a calcium-dependent manner. Blood **82:**1875–1883.
27. **Schiffmann, S. N., G. Cheron, A. Lohof, P. d'Alcantara, M. Meyer, M. Parmentier, and S. Schurmans.** 1999. Impaired motor coordination and Purkinje cell excitability in mice lacking calretinin. Proc. Natl. Acad. Sci. USA **96:**5257–5262.
28. **Selinfreund, R. H., S. W. Barger, M. J. Welsh, and L. J. Van Eldik.** 1990. Antisense inhibition of glial S100 beta production results in alterations in cell morphology, cytoskeletal organization, and cell proliferation. J. Cell Biol. **111:**2021–2028.
29. **Sengelov, H., L. Kjeldsen, M. S. Diamond, T. A. Springer, and N. Borregaard.** 1993. Subcellular localization and dynamics of Mac-1 (alpha m beta 2) in human neutrophils. J. Clin. Investig. **92:**1467–1476.
30. **Srikrishna, G., K. Panneerselvam, V. Westphal, V. Abraham, A. Varki, and H. H. Freeze.** 2001. Two proteins modulating transendothelial migration of leukocytes recognize novel carboxylated glycans on endothelial cells. J. Immunol. **166:**4678–4688.
31. **Sun, H. Q., M. Yamamoto, M. Mejillano, and H. L. Yin.** 1999. Gelsolin, a multifunctional actin regulatory protein. J. Biol. Chem. **274:**33179–33182.
32. **van den Bos, C., J. Roth, H. G. Koch, M. Hartmann, and C. Sorg.** 1996. Phosphorylation of MRP14, an S100 protein expressed during monocytic differentiation, modulates Ca(2+)-dependent translocation from cytoplasm to membranes and cytoskeleton. J. Immunol. **156:**1247–1254.
33. **Xiong, Z., D. O'Hanlon, L. E. Becker, J. Roder, J. F. MacDonald, and A. Marks.** 2000. Enhanced calcium transients in glial cells in neonatal cerebellar cultures derived from S100B null mice. Exp. Cell. Res. **257:**281–289.